Electrochemistry of Free Chlorine and Monochloramine and its Relevance to the Presence of Pb in Drinking Water

ARTICLE *in* ENVIRONMENTAL SCIENCE AND TECHNOLOGY · JULY 2007

Impact Factor: 5.33 · DOI: 10.1021/es062922t · Source: PubMed

4 AUTHORS, INCLUDING:

Vishnu Rajasekharan
Colorado State University
5 PUBLICATIONS **115** CITATIONS

SEE PROFILE

Jay A. Switzer
Missouri University of Science and Technology
123 PUBLICATIONS **3,370** CITATIONS

SEE PROFILE

Electrochemistry of Free Chlorine and Monochloramine and its Relevance to the Presence of Pb in Drinking Water

VISHNU V. RAJASEKHARAN, BRANDI N. CLARK, SANSANEE BOONSALEE, AND JAY A. SWITZER*

Department of Chemistry and Graduate Center for Materials Research, University of Missouri—Rolla, Rolla, Missouri 65409-117

The commonly used disinfectants in drinking water are free chlorine (in the form of HOCl/OCl^-) and monochloramine (NH_2Cl). While free chlorine reacts with natural organic matter in water to produce chlorinated hydrocarbon byproducts, there is also concern that NH_2Cl may react with Pb to produce soluble Pb(II) products—leading to elevated Pb levels in drinking water. In this study, electrochemical methods are used to compare the thermodynamics and kinetics of the reduction of these two disinfectants. The standard reduction potential for NH_2Cl/Cl^- was estimated to be +1.45 V in acidic media and +0.74 V in alkaline media versus NHE using thermodynamic cycles. The kinetics of electroreduction of the two disinfectants was studied using an Au rotating disk electrode. The exchange current densities estimated from Koutecky—Levich plots were 8.2×10^{-5} and 4.1×10^{-5} A/cm^2, and by low overpotential experiments were $7.5 \pm 0.3 \times 10^{-5}$ and $3.7 \pm 0.4 \times 10^{-5}$ A/cm^2 for free chlorine and NH_2Cl, respectively. The rate constant for the electrochemical reduction of free chlorine at equilibrium is approximately twice as large as that for the reduction of NH_2Cl. Equilibrium potential measurements show that free chlorine will oxidize Pb to PbO_2 above pH 1.7, whereas NH_2Cl will oxidize Pb to PbO_2 only above about pH 9.5, if the total dissolved inorganic carbon (DIC) is 18 ppm. Hence, NH_2Cl is not capable of producing a passivating PbO_2 layer on Pb, and could lead to elevated levels of dissolved Pb in drinking water.

Introduction

Free chlorine (in the form of hypochlorous acid (HOCl) and hypochlorite anion (OCl^-)) and monochloramine (NH_2Cl) have been used as disinfectants in drinking water (*1*). They both, however, produce disinfection byproducts. Free chlorine reacts with organic compounds present in water to produce chlorinated hydrocarbons such as trihalomethanes, which are suspected to be carcinogens (*2*). There is also evidence that NH_2Cl reacts with Pb present in lead service lines, solder, and brass to form soluble Pb(II) (*3*−*6*). As a consequence, it is important to understand the difference in reactivity of these two disinfectants to ensure the safety of drinking water.

* Corresponding author phone: (573) 341-4383; fax: (573) 341-2071; e-mail: jswitzer@umr.edu.

In our earlier work, we showed that NH_2Cl oxidized Pb to soluble Pb(II) species, whereas free chlorine produced a passivating layer of PbO_2 on the Pb (*3*). Previous theoretical studies (*3*, *7*−*10*) showed that both NH_2Cl and free chlorine are capable of oxidizing Pb to PbO_2, based on the standard reduction potential. However, in real systems only free chlorine forms PbO_2, whereas NH_2Cl forms Pb(II) species (*3*−*6*, *11*, *12*).

The chemical reactivity (*9*, *13*−*26*) and the electroactivity (*27*−*32*) of these disinfectants have been studied by other workers. For example, Valentine and co-workers have studied the mechanistic aspects of the reactions between NH_2Cl and Fe(II) in aqueous solutions (*15*−*17*). They have presented evidence that the oxidation of Fe(II) to Fe(III) by monochloramine occurs through the formation of a reactive intermediate (amidogen radical ($NH_2^\bullet$)) via two sequential one-electron steps (*15*). Wrona and Piela studied the electroreduction of chloramines on rotating Pt and Au electrodes (*27*). They also suggest that the electroreduction of monochloramine occurs via the formation of amidogen radical.

In the present work, we use electrochemical measurements to provide a direct comparison of the kinetics and thermodynamics of the electron-transfer reactions of free chlorine and NH_2Cl. The thermodynamics of the reduction of the two disinfectants is compared by calculating the standard reduction potentials from thermodynamic cycles, and by performing equilibrium (i.e., open-circuit) potential measurements. The chemical reversibility and redox activity of the two disinfectants is probed in unstirred solution by cyclic voltammetry. The kinetics of reduction of the two disinfectants is studied using a Au rotating disk electrode (RDE). The RDE is used to control mass transport to the electrode, so that the kinetics can be separated from mass transport by using Koutecky−Levich analysis. Finally, the equilibrium potentials of free chlorine and NH_2Cl are plotted on a Pourbaix diagram for the Pb−H_2O−CO_2 system in order to understand the effects of the two disinfectants on the dissolution of Pb.

Experimental Section

All experiments were conducted using deionized 18 MΩ-cm water from a Barnstead NANOpure ultrapure water system. A sodium hypochlorite (NaOCl) solution with 10−13 vol % available chlorine was used as a source for free chlorine. NH_2Cl and free chlorine solutions were prepared fresh for each experiment. Free chlorine and NH_2Cl have characteristic UV absorption bands. The actual concentrations of OCl^- (at pH 9 the predominant species of free chlorine is OCl^- (97%)) and NH_2Cl were determined spectrophotometrically at 292 nm ($\epsilon = 350$ M^{-1} cm^{-1}) (*21*) and 243 nm ($\epsilon = 461$ M^{-1} cm^{-1}) (*21*), respectively. The concentration of $NHCl_2$ was determined at 206 nm ($\epsilon = 2100$ M^{-1} cm^{-1}) (*27*).

The NH_2Cl solutions were prepared by reacting free chlorine with a 5-fold molar excess of aqueous NH_3. The excess NH_3 minimizes the formation of dichloramine ($NHCl_2$) (*33*). To prepare the NH_2Cl solutions, 5 mL of 100 mM NH_3 was added to a rapidly stirred 20 mL solution of 5 mM NaOCl. The solutions for kinetic studies were buffered at pH 9 with 60 mM $NaHCO_3$. The supporting electrolyte was 100 mM Na_2SO_4. For the equilibrium potential measurements, 60 mM NaH_2PO_4 was used as a buffer for pH 7−8, and 60 mM $NaHCO_3$ or H_3BO_3 were used as buffers in the pH range of 9−12. It is important to note that these buffers can be used to study the electrochemistry of NH_2Cl and free chlorine on inert electrodes such as Au or Pt, but they would complicate studies involving Pb or PbO_2 elec-

trodes because of the formation of insoluble Pb(II) carbonates and phosphates.

A Fisher Scientific Accumet model 15 digital pH meter equipped with an Accumet combination electrode was used for the pH measurements. An Accumet chloride combination ion selective electrode was used to measure the chloride ion concentration. A Hach ammonia gas sensing combination electrode was used to measure the total excess ammonia present in the NH_2Cl containing solutions. Typically, approximately 4 mM total ammonia was present after the formation of NH_2Cl.

Electrochemical experiments were performed using a Brinkmann PGSTAT 100 potentiostat controlled by GPES software v. 4.9. The experiments were run at room temperature in a cell that was not thermostatted. A polycrystalline Au electrode (Pine Instruments, USA) of geometric area 0.196 cm^2 was used for stationary and rotating disk studies. A MSRX speed controller from Pine instrument company was used to vary the rotation rates. The counter electrode was a Pt wire. A saturated calomel electrode (SCE) was used as the reference electrode in all electrochemical experiments. All potentials, except equilibrium potentials, are reported versus the SCE. The equilibrium potentials are reported versus the normal hydrogen electrode (NHE) by adding 0.242 V to the potential measured versus SCE. The equilibrium potentials were measured on an Au electrode after equilibrating for 1000 s. Equilibrium potentials must be measured with a high impedance voltmeter or electrometer, so that the equilibrium is not shifted by current flow. In our studies the Brinkmann PGSTAT 100 potentiostat (input impedance greater than 100 G ohm) was used for these measurements. The working solutions were deoxygenated by bubbling with argon (99.998%)(BOC gases).

Results and Discussion

Calculation of the Standard Reduction Potential of NH_2Cl. The standard reduction potential of the NH_2-Cl/Cl^- couple in both acidic and alkaline solutions can be estimated using the following parameters: the equilibrium constants for eqs 1 (*20*), 2, 4, and 5 and the standard reduction potentials for $HOCl/Cl^-$ and OCl^-/Cl^-, (eqs 3 and 6) (*34*). The relationship between the free energy, equilibrium constant and standard reduction potential ($\Delta G^\circ = -RT \ln K = -nFE^\circ$) was then used to calculate the ΔG° for the reactions below. By convention, the equilibrium constants are shown without units, although they are based on molar concentrations.

$$NH_2Cl + H_2O \leftrightarrows NH_3 + HOCl \quad K = 2.63 \times 10^{-11}; \quad \Delta G1^\circ = 60 \text{ kJ/mol} \quad (1)$$

$$NH_3 + H^+ \leftrightarrows NH_4^+ \quad K = 1.78 \times 10^9; \quad \Delta G2^\circ = -53 \text{ kJ/mol} \quad (2)$$

$$HOCl + H^+ + 2e^- \leftrightarrows Cl^- + H_2O \quad E^\circ = +1.482 \text{ V}; \quad \Delta G3^\circ = -286 \text{ kJ/mol} \quad (3)$$

$$HOCl \leftrightarrows OCl^- + H^+ \quad K = 2.9 \times 10^{-8}; \quad \Delta G4^\circ = 43 \text{ kJ/mol} \quad (4)$$

$$H^+ + OH^- \leftrightarrows H_2O \quad K = 5.56 \times 10^{15}; \quad \Delta G5^\circ = -90 \text{ kJ/mol} \quad (5)$$

$$OCl^- + H_2O + 2e^- \leftrightarrows Cl^- + 2OH^- \quad E^\circ = +0.81 \text{ V}; \quad \Delta G6^\circ = -156 \text{ kJ/mol} \quad (6)$$

The standard reduction potentials of NH_2Cl in acidic and alkaline solutions can be determined by standard thermodynamic cycles. To estimate ΔG_a° for the reduction reaction of NH_2Cl in acidic media (i.e., pH = 0), the ΔG°s for the elementary reactions shown in eqs 1, 2, and 3 are summed, as shown in eq 7.

$$\Delta Ga^\circ = \Delta G1^\circ + \Delta G2^\circ + \Delta G3^\circ = -279 \text{ kJ/mol} \quad (7)$$

From eq 7 the standard reduction potential for NH_2Cl can be determined, and is given below in eq 8

$$NH_2Cl + 2H^+ + 2e^- \leftrightarrows Cl^- + NH_4^+ \quad E^\circ = +1.45 \text{ V vs NHE} \quad (8)$$

To estimate ΔG_b° for the reduction reaction of NH_2Cl in alkaline media (i.e., pH = 14), the ΔG°s for the elementary reactions shown in eqs 1, 4, 5, and 6 are summed, as shown in eq 9.

$$\Delta Gb^\circ = \Delta G1^\circ + \Delta G4^\circ + \Delta G5^\circ + \Delta G6^\circ = -143 \text{ kJ/mol} \quad (9)$$

From eq 9 the standard reduction potential for NH_2Cl can be determined, and is given below in eq 10

$$NH_2Cl + H_2O + 2e^- \leftrightarrows Cl^- + OH^- + NH_3 \quad E^\circ = +0.74 \text{ V vs NHE} \quad (10)$$

Equilibrium Potentials for NH_2Cl. Equilibrium (i.e., open-circuit) potential measurements for NH_2Cl were performed on a Au electrode in solutions containing equimolar quantities of the redox species in 60 mM buffered solutions. Equilibrium potentials are also referred to in the literature as oxidation−reduction potentials (ORPs). James et al. have previously used ORP measurements to compare the relative impact of various disinfectants on metallic plumbing material solubility and speciation (*35*). Figure 1 shows a plot of the measured (open circles) equilibrium potentials for NH_2Cl as a function of pH. Figure 1 also compares the measured equilibrium potentials to calculated formal potentials. The standard reduction potentials for eqs 8 and 10 are for all of the reactants and products at unit activity. Formal potentials for these reactions at other concentrations and pHs can be calculated from the Nernst equation (eq 11).

$$E = E^\circ - RT/nF \ln Q \quad (11)$$

where E is the formal potential (V), E° is the standard reduction potential (V), R is the molar gas constant (8.314 J $mol^{-1} K^{-1}$), T is the absolute temperature (K), n is the number of electrons transferred, F is Faraday's constant (96 485 C), and Q is the reaction quotient (dimensionless).

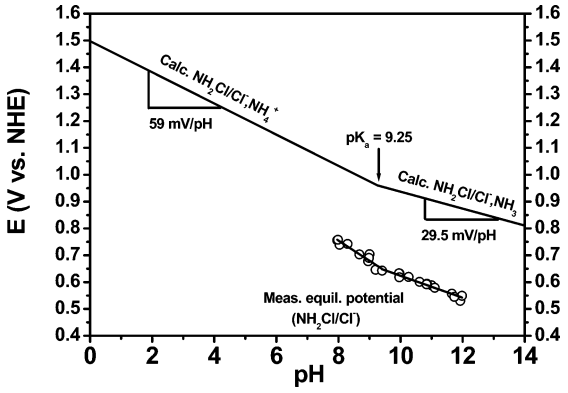

FIGURE 1. Measured equilibrium potentials (shown as open circles) for the NH_2Cl/Cl^- couple as a function of pH. A linear fit to the measured equilibrium potentials gives two linear regions. Below pH 9.4 the slope is 75 mV/pH, and above pH 9.4 the slope is 41 mV/pH. Calculated formal potentials from the Nernst equation are also shown as solid lines, which change slope at a pH of 9.25, corresponding to the pK_a of NH_4^+.

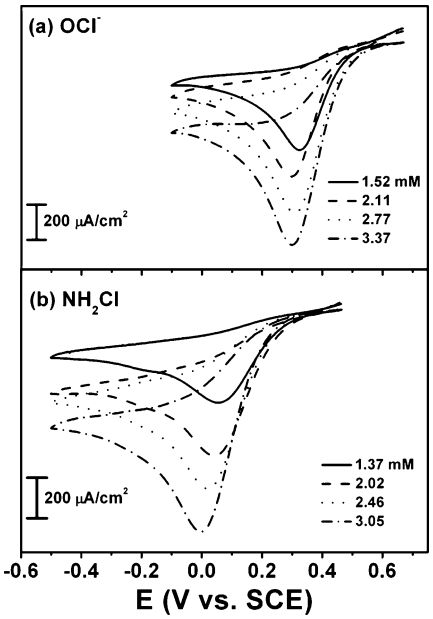

FIGURE 2. Cyclic voltammograms for the reduction of (a) OCl^- and (b) NH_2Cl on a stationary Au electrode at a scan rate of 50 mV/s. The CVs were run in unstirred solutions of OCl^- and NH_2Cl of various concentrations. The pH 9 solutions were Ar purged, and contained 0.1 M Na_2SO_4 and 60 mM $NaHCO_3$.

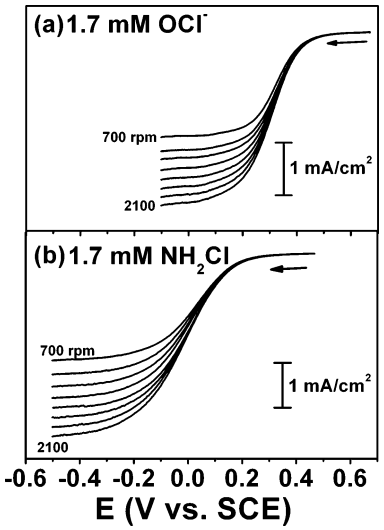

FIGURE 3. Linear sweep voltammograms of 1.7 mM (a) OCl^- and (b) NH_2Cl on a Au rotating disk electrode at rotation rates from 700 to 2100 rpm. The voltammograms were run at a sweep rate of 50 mV/s in Ar-purged solutions containing 0.1 M Na_2SO_4, 60 mM $NaHCO_3$ at pH 9.

The formal reduction potentials (solid lines) calculated from eq 11 are shown in Figure 1. The formal potentials were calculated from eq 11 with $[NH_2Cl] = [Cl^-] = 1$ mM, and $[NH_3] + [NH_4^+] = 4$ mM. For the calculated formal potentials, a Nernstian slope of 59 mV/pH is predicted at low pH, and a slope of 29.5 mV/pH is predicted at high pH. The change in slope at pH 9.25 is due to the fact that NH_4^+ ($pK_a = 9.25$) is formed below the pK_a, and NH_3 is formed above the pK_a. The slope of a linear fit for the values of measured equilibrium potentials is 75 mV/pH below pH 9.4 and 41 mV/pH above pH 9.4.

The measured equilibrium potential is approximately 300 mV more negative than the calculated formal potential at pH 9.25. This suggests that there is either an error in the calculated standard reduction potentials for eqs 8 and 10

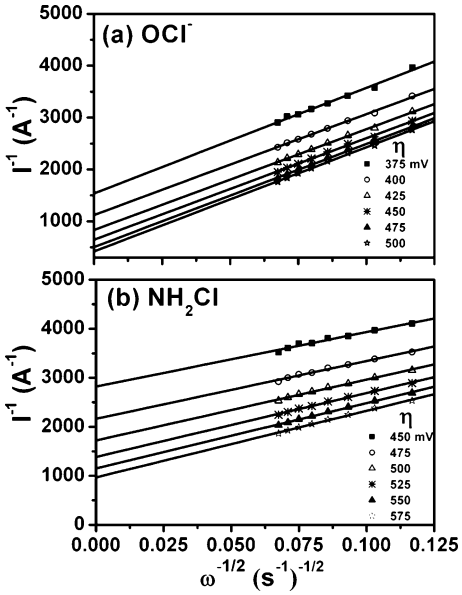

FIGURE 4. Koutecky–Levich plots for 1.7 mM (a) OCl^- and (b) NH_2Cl at a series of different overpotentials (η). Open circuit values of 0.67 V for OCl^- and 0.47 V for NH_2Cl were used to approximate the overpotentials for determining the kinetic currents (i_k).

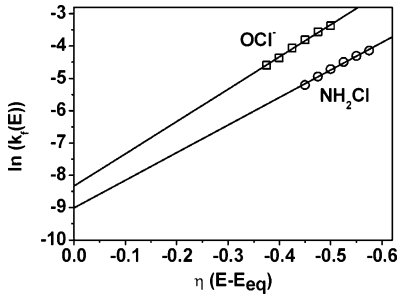

FIGURE 5. Plots of ln $k_f(E)$ versus overpotential (η) for the data obtained from the Koutecky–Levich plots shown in Figure 4. The intercept of the linear fits is ln (k°), and the slope is proportional to the transfer coefficient (α).

due to an error in the equilibrium constant for eq 1 (*9*, *36*), or that the reduction of NH_2Cl does not proceed by the reactions shown in eqs 8 and 10. One explanation is that there are competing reactions involving reactive amidogen ($NH_2^\bullet$) radical intermediates. The radicals could either couple to produce hydrazine or react with bicarbonate in solution. In either case, the measured equilibrium potential would be different from the calculated formal potential. Valentine and co-workers have shown evidence for the formation of the amidogen radical during oxidation of Fe(II) (*15*). They have also proposed that these radicals can be scavenged by bicarbonate or that radical–radical coupling can occur to produce hydrazine. Piela and Wrona have also suggested that the amidogen radical is produced in the rate determining, one-electron step during the electroreduction of NH_2Cl (*27*).

Cyclic Voltammetry of OCl- and NH_2Cl. Figure 2a and b show cyclic voltammograms (CVs) of (a) OCl^- and (b) NH_2Cl in Ar-purged solutions containing 60 mM $NaHCO_3$ and 0.1 M Na_2SO_4 at pH 9 for various concentrations of the two disinfectants. The CVs were run in an unstirred solution at a scan rate of 50 mV/s on a Au stationary electrode. In the CVs, OCl^- and NH_2Cl both show single cathodic peaks at approximately 0.32 and 0.03 V, respectively. There are no significant anodic peaks corresponding to these cathodic peaks, showing that the reactions are electrochemically irreversible reductions. In oxygen-saturated solutions (not shown), both solutions show an additional cathodic peak at

TABLE 1. Comparison of the Kinetic Parameters Determined by the Koutecky–Levich and Low Overpotential Methods for the Electrochemical Reduction of NH_2Cl and OCl^-

	Koutecky–Levich plot			low overpotential plot	
species	j_o (A/cm^2)	k° (cm/s)	α	j_o (A/cm^2)	k° (cm/s)
NH_2Cl	4.1×10^{-5}	1.2×10^{-4}	0.2	$3.7 \pm 0.4 \times 10^{-5}$	$1.1 \pm 0.1 \times 10^{-4}$
OCl^-	8.2×10^{-5}	2.5×10^{-4}	0.3	$7.5 \pm 0.3 \times 10^{-5}$	$2.3 \pm 0.1 \times 10^{-4}$

−0.25 V due to the reduction of dissolved oxygen. The cathodic peak currents for the reduction of both OCl^- and NH_2Cl increase linearly as the concentrations of the two disinfectants are increased.

Rotating Disk Studies of the Reduction of OCl^- and NH_2Cl. The standard heterogeneous rate constant (k°) for the reduction of OCl^- and NH_2Cl can be determined at the equilibrium potential (i.e., zero driving force) using the rotating disk electrode by both Koutecky–Levich analysis, and by using a linear approximation to the Butler–Volmer equation at very low overpotential (*37*). Figure 3a and b show linear sweep voltammograms of 1.7 mM OCl^- and NH_2Cl, respectively, in an Ar-purged solution containing 60 mM $NaHCO_3$ and 0.1 M Na_2SO_4 at pH 9 at a scan rate of 50 mV/s on a Au rotating disk electrode at various rotation rates. Both disinfectants show mixed kinetic-diffusion regimes at intermediate potentials and mass-transport-limited currents at high overpotentials. Koutecky–Levich analysis was done in the mixed kinetic-diffusion regimes. The Koutecky–Levich equation is shown in eq 12.

$$\frac{1}{i} = \frac{1}{i_k} + \frac{1}{i_l} = \frac{1}{i_k} + \frac{1}{0.62nFAD^{2/3}\omega^{1/2}\upsilon^{-1/6}C} \qquad (12)$$

where i is the measured current (A), i_k is the current in the absence of any mass-transport effects (A), i_l is the limiting current at high overpotential (A), n is the number of electrons transferred, F is Faraday's constant (96 485 C), A is the electrode area (cm^2), D is the diffusion coefficient (cm^{2}s^{-1}), ω is the angular frequency of rotation (s^{-1}), υ is the kinematic viscosity (cm^{2}s^{-1}), and C is the concentration (mol/cm^3).

Figure 4 shows Koutecky–Levich plots of $1/i$ versus $1/\omega^{1/2}$ for (a) OCl and (b) NH_2Cl at a series of overpotentials (η). The overpotentials were approximated by taking the difference between the applied electrode potential and the open circuit potentials of 0.67 V for OCl^- and 0.47 V for NH_2Cl. Straight lines are observed for both disinfectants with intercepts corresponding to their kinetic currents (i_k) for a wide range of overpotentials (0.375–0.575 V). The kinetic currents (i_k) can be converted to rate constants (k_f) using eq 13.

$$i_k = nFAk_fC \qquad (13)$$

where n is the number of electrons transferred, F is Faraday's constant (C), A is the electrode area (cm^2), k_f is the forward rate constant (cm/s), and C is the concentration (mol/cm^3). We assumed $n = 2$ for these calculations.

Figure 5 shows a plot of ln $k_f(E)$ versus overpotential (η). This plot should have a slope of $-\alpha F/RT$ and an intercept equal to ln (k°) (*37*). The α value determined from the slope for OCl^- was 0.3, and for NH_2Cl was 0.2. The k° value obtained for OCl^- was 2.5×10^{-4} cm/s and, for NH_2Cl was 1.2×10^{-4} cm/s. The exchange current densities (j_o) determined from these k° values using eq 13 and normalizing for the electrode area were 8.2×10^{-5} and 4.1×10^{-5} A/cm^2 for OCl^- and NH_2Cl, respectively. These values show that, at equilibrium, the rate constant for the reduction of OCl^- is approximately twice that of NH_2Cl.

The standard heterogeneous rate constant k° can also be estimated from linear sweep voltammograms at low overpotential, where mass-transport effects are minimal. For small values of overpotential, η, the Butler–Volmer equation is approximated by eq 14 (*37*, *38*).

$$j = \frac{-j_oF\eta}{RT} \qquad (14)$$

where j is the measured current density (A/cm^2), j_o is the exchange current density (A/cm^2), F is Faraday's constant (C), η is the applied overpotential (V), R is the molar gas constant (J mol^{-1} K^{-1}), and T is the absolute temperature ($F/RT = 38.92$ V^{-1} at 298 K). Figure 6 shows plots of j versus η for 1.7 mM OCl^- and NH_2Cl in an Ar-purged solution containing 60 mM $NaHCO_3$ and 0.1 M Na_2SO_4 at pH 9. The

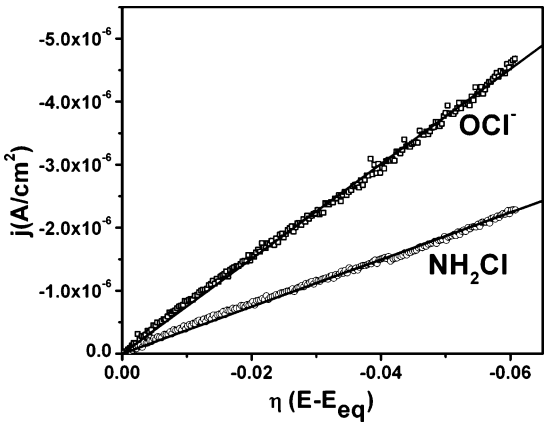

FIGURE 6. Plots of current density (j) versus overpotential (η) in the small overpotential range (0–60 mV) for OCl^- and NH_2Cl at a rotation rate of 900 rpm in an Ar-purged solution containing 0.1 M Na_2SO_4, 60 mM $NaHCO_3$ at pH 9. The scan rate was 1 mV/s.

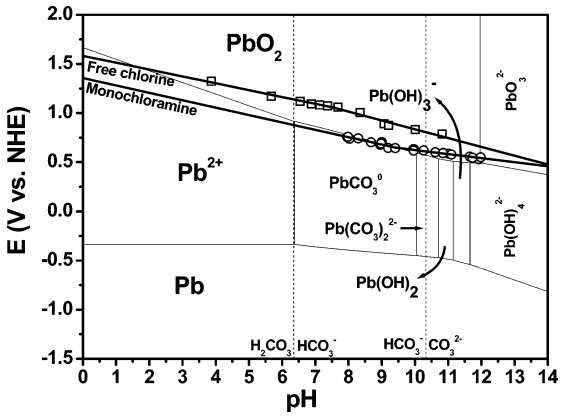

FIGURE 7. Pourbaix diagram for Pb–H_2O–CO_2 system with the concentration of dissolved Pb species equal to 7.25×10^{-8} M (15 ppb) and the concentration of dissolved inorganic carbon equal to 1.5×10^{-3} M (18 ppm) at 25 °C. Measured equilibrium potentials are shown as open squares for free chlorine, and as open circles for NH_2Cl. A linear fit to the measured equilibrium potentials for free chlorine gives two linear regions. Below pH 7.5 (corresponding to the pK_a = 7.5 of HOCl) the slope is 70 mV/pH, and above pH 7.5 the slope is 90 mV/pH.

voltammograms were run at a scan rate of 1 mV/s on a Au electrode at 900 rpm. The slopes of the j versus η plots for the disinfectants were not dependent on the rotation rate. The slopes of five different rotation rates (700, 900, 1100, 1300, and 1500 rpm) were obtained to estimate the error involved in the measurements. The exchange current densities, j_o, determined from these slopes are $7.5 \pm 0.3 \times 10^{-5}$ A/cm^2 for OCl^- and $3.7 \pm 0.4 \times 10^{-5}$ A/cm^2 for NH_2Cl. The k° values determined from the j_o values are $2.3 \pm 0.1 \times 10^{-4}$ and $1.1 \pm 0.1 \times 10^{-4}$ cm/s for OCl^- and NH_2Cl, respectively.

The exchange current densities and standard heterogeneous rate constant for OCl^- and NH_2Cl are summarized in Table 1 for measurement by both Koutecky−Levich analysis and by the linear approximation of the Butler−Volmer equation at low overpotential. Both methods show that at equilibrium (zero driving force), the rate constant for the reduction of OCl^- is approximately twice that of NH_2Cl.

Measured Equilibrium Potential as a Diagnostic Tool to Determine the Stability of Pb. Figure 7 shows the Pourbaix diagram for the Pb−H_2O−CO_2 system along with the measured formal potentials of NH_2Cl and free chlorine. This diagram is constructed to determine the stability of Pb in the presence of these disinfectants. Figure 7 is similar to the one constructed by Schock and co-workers (*39*−*41*). The concentration of the dissolved Pb(II) species in Figure 7 is fixed at the action level of Pb in drinking water (7.2×10^{-8} M) (15 ppb). The concentration of total dissolved inorganic carbon (DIC) is chosen as 1.5 mM (18 ppm), which is the value previously used by Schock et al. (*40*). The Gibbs free energies of formation of the different Pb species at 298 K and 1 atm are used to calculate the equilibrium constants and standard reduction potentials for the chemical and electrochemical reactions of different Pb species (*41*). The lead carbonate species are included in Figure 7, due to the importance of carbonate compounds of the Pb(II) species (*41*−*44*). In our previous study we observed a lead carbonate phase (hydrocerrusite ($Pb_3(CO_3)_2(OH)_2$)), when a Pb film was exposed to a solution containing NH_2Cl (*3*).

In Figure 7, the measured equilibrium potentials for NH_2Cl/Cl^- are more negative than those of the free chlorine species for pH values that are relevant to drinking water. This is a direct indication that NH_2Cl is a thermodynamically weaker oxidizing agent than free chlorine. Figure 7 shows that free chlorine is thermodynamically capable of oxidizing Pb to PbO_2 above pH 1.7, whereas NH_2Cl is thermodynamically capable of oxidizing Pb to PbO_2 only above about pH 9.5 at the DIC level of 18 ppm. Even above pH 9.5, the driving force for the production of PbO_2 by NH_2Cl is small. It is also dependent on the concentration of Pb(II) used to calculate the Pourbaix diagram, and on the concentration of dissolved inorganic carbon. The relationship of the measured equilibrium potentials with the Pb(II)/PbO_2 boundary in the Pourbaix diagram is consistent with our previous *in-situ* Pb dissolution studies at pH 8, in which NH_2Cl oxidizes Pb to Pb(II) species such as $Pb_3(CO_3)_2(OH)_2$, whereas free chlorine oxidizes Pb to insoluble, tetravalent PbO_2 (*3*). The measurement of equilibrium potentials in drinking water may prove to be a useful diagnostic tool to determine the stability of Pb in the presence of these disinfectants.

Acknowledgments

This work was supported by NSF grants CHE-0437346 and DMR-0504715.

Literature Cited

(1) White, G. C. *Handbook of Chlorination and Alternative Disinfectants*, 2nd ed.; Van Nostrand Reinhold Company: New York, 1986.
(2) U.S. Environmental Protection Agency. National interim primary drinking water regulations; control of trihalomethanes in drinking water. *Fed. Regist.* **1979**, *44*, 68624−68707.
(3) Switzer, J. A.; Rajasekharan, V. V.; Boonsalee, S.; Kulp, E. A.; Bohannan, E. W. Evidence that Monochloramine Disinfectant Could Lead to Elevated Pb Levels in Drinking Water. *Environ. Sci. Technol.* **2006**, *40*, 3384−3387.
(4) Edwards, M.; Dudi, A. Role of chlorine and chloramine in corrosion of lead-bearing plumbing materials. *J. Am. Water Works Assoc.* **2004**, *96*, 69−81.
(5) Renner, R. Plumbing the depths of D.C.'s drinking water crisis. *Environ. Sci. Technol.* **2004**, *38*, 224A−227A.
(6) Renner, R. Chloramines again linked to lead in drinking water. *Environ. Sci. Technol.* **2005**, *39*, 314A.
(7) Jolly, W. L. The thermodynamic properties of chloramine, dichloramine, and nitrogen trichloride. *J. Phys. Chem.* **1956**, *60*, 507−508.
(8) Soulard, M.; Bloc, F.; Hatterer, A. Diagrams of existence of chloroamines and bromoamines in aqueous solution. *J. Chem. Soc., Dalton Trans.* **1981**, 2300−2310.
(9) Gray, E. T., Jr.; Margerum, D. W.; Huffman, R. P. Chloramine equilibriums and the kinetics of disproportionation in aqueous solution. *ACS Symp. Ser.* **1978**, *82*, 264−277.
(10) Wrona, P. K. Electrode processes of chloramines in aqueous solutions. *J. Electroanal. Chem.* **1998**, *453*, 197−204.
(11) Renner, R. More chloramine complications. *Environ. Sci. Technol.* **2004**, *38*, 342A−343A.
(12) Renner, R. Chloramine's effect on lead in drinking water. *Environ. Sci. Technol.* **2006**, *40*, 3129−3130.
(13) Yiin, B. S.; Margerum, D. W. Non-metal redox kinetics: reactions of trichloramine with ammonia and with dichloramine. *Inorg. Chem.* **1990**, *29*, 2135−2141.
(14) Yiin, B. S.; Walker, D. M.; Margerum, D. W. Nonmetal redox kinetics: general-acid-assisted reactions of chloramine with sulfite and hydrogen sulfite. *Inorg. Chem.* **1987**, *26*, 3435−3441.
(15) Vikesland, P. J.; Valentine, R. L. Reaction Pathways Involved in the Reduction of Monochloramine by Ferrous Iron. *Environ. Sci. Technol.* **2000**, *34*, 83−90.
(16) Vikesland, P. J.; Valentine, R. L. Iron Oxide Surface-Catalyzed Oxidation of Ferrous Iron by Monochloramine: Implications of Oxide Type and Carbonate on Reactivity. *Environ. Sci. Technol.* **2002**, *36*, 512−519.
(17) Vikesland, P. J.; Valentine, R. L. Modeling the kinetics of ferrous iron oxidation by monochloramine. *Environ. Sci. Technol.* **2002**, *36*, 662−668.
(18) Snyder, M. P.; Margerum, D. W. Kinetics of chlorine transfer from chloramine to amines, amino acids, and peptides. *Inorg. Chem.* **1982**, *21*, 2545−2550.
(19) Margerum, D. W.; Gray, E. T., Jr.; Huffman, R. P. Chlorination and the formation of N-chloro compounds in water treatment. *ACS Symp. Ser.* **1978**, *82*, 278−291.
(20) Margerum, D. W.; Schurter, L. M.; Hobson, J.; Moore, E. E. Water chlorination chemistry: nonmetal redox kinetics of chloramine and nitrite ion. *Environ. Sci. Technol.* **1994**, *28*, 331−337.
(21) Kumar, K.; Day, R. A.; Margerum, D. W. Atom-transfer redox kinetics: general-acid-assisted oxidation of iodide by chloramines and hypochlorite. *Inorg. Chem.* **1986**, *25*, 4344−4350.
(22) Kumar, K.; Margerum, D. W. Kinetics and mechanism of general-acid-assisted oxidation of bromide by hypochlorite and hypochlorous acid. *Inorg. Chem.* **1987**, *26*, 2706−2711.
(23) Gerritsen, C. M.; Margerum, D. W. Non-metal redox kinetics: hypochlorite and hypochlorous acid reactions with cyanide. *Inorg. Chem.* **1990**, *29*, 2757−2762.
(24) Fogelman, K. D.; Walker, D. M.; Margerum, D. W. Nonmetal redox kinetics: hypochlorite and hypochlorous acid reactions with sulfite. *Inorg. Chem.* **1989**, *28*, 986−993.
(25) Dodd, M. C.; Vu, N. D.; Ammann, A.; Le, V. C.; Kissner, R.; Pham, H. V.; Cao, T. H.; Berg, M.; von Gunten, U. Kinetics and Mechanistic Aspects of As(III) Oxidation by Aqueous Chlorine, Chloramines, and Ozone: Relevance to Drinking Water Treatment. *Environ. Sci. Technol.* **2006**, *40*, 3285−3292.
(26) Conocchioli, T. J.; Hamilton, E. J., Jr.; Sutin, N. Formation of iron(IV) in the oxidation of iron(II). *J. Am. Chem. Soc.* **1965**, *87*, 926−927.
(27) Piela, B.; Wrona, P. K. Electrochemical Behavior of Chloramines on the Rotating Platinum and Gold Electrodes. *J. Electrochem. Soc.* **2003**, *150*, E255−E265.
(28) Kishioka, S.-y.; Kosugi, T.; Yamada, A. Electrochemical Determination of a Free Chlorine Residual Using Cathodic Potential-Step Chronocoulometry. *Electroanalysis* **2005**, *17*, 724−726.

(29) Marks, H. C.; Bannister, G. L.; Glass, J. R.; Herrigel, E. Amperometric methods in the control of water chlorination. *Anal. Chem.* **1947**, *19*, 200−204.
(30) Jenkins, E. N. Reactions of hypochlorous acid and sodium hypochlorite at the dropping-mercury electrode. *J. Chem. Soc.* **1951**, 2627−2630.
(31) Heller, K.; Jenkins, E. N. Behavior of hypochlorite and of N-chloroamines at the dropping-mercury electrode. *Nature (London, United Kingdom)* **1946**, *158*, 706.
(32) Evans, O. M. Voltammetric determination of the decomposition rates of combined chlorine in aqueous solution. *Anal. Chem.* **1982**, *54*, 1579−1582.
(33) Brodtmann, N. V., Jr.; Russo, P. J. The use of chloramine for reduction of trihalomethanes and disinfection of drinking water. *J. Am. Water Works Assoc.* **1979**, *71*, 40−42.
(34) Lide, D. R., Ed. *CRC Handbook of Chemistry and Physics*, 86th ed.; Taylor & Francis Group: New York, 2005−2006.
(35) James, C. N.; Copeland, R. C.; Lytle, D. A. Relationships between oxidation-reduction potential, oxidant, and pH in drinking water. In *Proceedings of the AWWA Water Quality Technology Conference*, San Antonio, Texas, November 14−18, 2004; pp 1−13.
(36) Anbar, M.; Yagil, G. The hydrolysis of chloramine in alkaline solution. *J. Am. Chem. Soc.* **1962**, *84*, 1790−1796.
(37) Bard, A. J.; Faulkner, L. R. *Electrochemical Methods: Fundamentals and Applications*, 2nd ed.; John Wiley & Sons: New York, 2001.
(38) Switzer, J. A.; Kothari, H. M.; Bohannan, E. W. Thermodynamic to Kinetic Transition in Epitaxial Electrodeposition. *J. Phys. Chem. B* **2002**, *106*, 4027−4031.
(39) Lytle, D. A.; Schock, M. R. The formation of Pb(IV) oxides in chlorinated water. *J. Am. Water Works Assoc.* **2005**, *97*, 102−114.
(40) Schock, M. R.; Harmon, S. M.; Swertfeger, J.; Lohmann, R. Tetravalent lead: a hitherto unrecognized control of tap water lead contamination. *Proc.-Water Quality Technol. Conf.* **2001**, 2270−2291.
(41) Schock, M. R.; Wagner, I.; Oliphant, R. J. In *Internal Corrosion of Water Distribution Systems*, 2nd ed.; AWWA: Denver, CO, 1996; pp 131−230.
(42) Schock, M. R. Response of lead solubility to dissolved carbonate in drinking water. *J. Am. Water Works Assoc.* **1980**, *72*, 695−704.
(43) Schock, M. R. Understanding corrosion control strategies for lead. *J. Am. Water Works Assoc.* **1989**, *81*, 88−100.
(44) Schock, M. R.; Gardels, M. C. Plumbosolvency reduction by high pH and low carbonate-solubility relationships. *J. Am. Water Works Assoc.* **1983**, *75*, 87−91

Received for review December 8, 2006. Revised manuscript received March 9, 2007. Accepted April 9, 2007.

ES062922T